concerned (cf. Table VII). In order to possibly identify the spectra associated with each of the five components observed at 77 K for the $^5D_0 \leftarrow {}^7F_0$ transition, we have recorded the luminescence spectra under variable-excitation and narrow-band-excitation conditions. The observed $^5D_0 \rightarrow {}^7F_1$ and $^5D_0 \rightarrow {}^7F_2$ transitions shown in Figures 8 and 9, respectively, reveal a unique property of the investigated compound. They display two features: (i) The number of components is larger than $2J + 1$; that is, each spectrum is the sum of several spectra originating from Eu(III) ions having different chemical environments. (ii) The general pattern of the spectra is largely dependent upon the excitation energy. The latter effect is particularly important for the $J = 1$ transition (Figure 8): some of its components have a small intensity in one spectrum, have a more intense one in the next, and then disappear. It is noteworthy that the lowest $^7F_1$ sublevel is shifted toward higher energy with decreasing excitation energy, whereas the other sublevels undergo a bathochromic shift larger than the shift in excitation energy. The $Me_2(2,2)$ compound therefore contains a wide dispersion of complex cation sites with a total crystal field splitting for $^7F_1$ ranging from 130 cm^{-1} ($\tilde{\nu}_{exc}$ = 17 250 cm^{-1}) to 250 cm^{-1} ($\tilde{\nu}_{exc}$ = 17 272 cm^{-1}). This may be again traced back to the large thermal motions of the macrocycle atoms evidenced by the room-temperature crystallographic study and generating several different conformations at 77 K. In view of the intensity distribution of the components of the transitions to $^7F_1$ and $^7F_2$, it appears that none of these conformations are clearly favored. Such a monotonous distribution of metal ion sites is analogous to what is observed in glasses.[23,55]

The above analysis of the emission spectra is confirmed by the lifetimes of the $^5D_0$ levels measured for both the hexanitrate and the complex cations. There is a large increase in the former in going from 293 to 77 K, consistent with the fact that most anions adopt a conformation with C_{2h} symmetry at low temperature. On the other hand, the average lifetime of the complex cations increases by 30% upon cooling, reflecting easy energy migration between the many cationic sites.

(55) Durville, F.; Boulon, G.; Reisfeld, R.; Mack, H.; Jørgensen, C. K. *Chem. Phys. Lett.* **1983**, *102*, 393.

Conclusion

This study confirms the complementarity of crystallographic and luminescence data for gaining information on the structure of materials containing disordered species. While the X-ray determination yields an average representation of the unit cell, the luminescence experiment allows one to probe the detailed local structure of the various moieties present in the microcrystalline material. In the investigated Eu compound, the $[Eu(NO_3)_2 \cdot Me_2(2,2)]^+$ cations adopt many different conformations, resulting in large but continuous variations in the crystal field splittings (>100 cm^{-1} for the total splitting of $^7F_1$). A somewhat similar situation has been observed for other macrocyclic compounds, the structures of which also display some degree of disorder. In the 18C6 complex,[33] the differences in the crystal field splittings were very small, amounting to a few wavenumbers only. In the complexes with the dicyclohexyl derivative of 18C6,[34] the luminescence spectra recorded under various excitation conditions presented large differences, but their components could be assigned to specific species with different conformations. For the presently investigated Eu complex, the various excitations produce luminescence spectra, the patterns of which vary in a monotonous way. This situation resembles that found in glasses. On the other hand, the $[Eu(NO_3)_6]^{3-}$ anions have a better defined structure, close to a C_{2h} arrangement at 77 K, and behave as microcrystals within this material.

Acknowledgment. This research is supported through grants from the Swiss National Science Foundation. We thank the Fondation Herbette (Lausanne, Switzerland) for the gift of spectroscopic equipment.

Supplementary Material Available: Atomic coordinates and isotropic thermal parameters for the Eu complex (Table S1), anisotropic parameters for the heavy atoms (Table S2) and selected least-squares weighted planes and dihedral angles for the Nd and Eu complexes (Table S5), luminescence spectra of the $[Eu(NO_3)_6]^{3-}$ anions under various excitation conditions (Figure F1), and luminescence spectra used in the determination of the site occupancies (Figure F2) (6 pages); observed structure factors for the Nd and Eu complexes (Tables S3 and S4, respectively) (52 pages). Ordering information is given on any current masthead page.

Contribution from the Department of Chemistry, University of Calgary, 2500 University Drive NW, Calgary, Alberta, Canada T2N 1N4

Structural Investigations on Tris(tetrahydrothiophene)rhodium(III) Halide Complexes

Peter D. Clark,* John H. Machin, John F. Richardson, Norman I. Dowling, and James B. Hyne

Received February 24, 1988

Complexes of the type $RhX_3(tht)_3$ (X = Cl, Br, I; tht = tetrahydrothiophene) were prepared and were studied by NMR spectroscopy and X-ray crystallography (X = Cl). The crystals of $RhCl_3(tht)_3$ are monoclinic and belong to the space group $P2_1/n$, with a = 11.887 (2) Å, b = 10.317 (1) Å, c = 15.237 (3) Å, β = 107.266 (9)°, V = 1784.4 (5) Å^3, and Z = 4. The structure was refined to give final agreement factors of R = 0.027 and R_w = 0.034 and showed that the complex adopts a meridional configuration. Rh–S bond lengths and other structural parameters were consistent with σ-bonding between the Rh atom and thioether ligands. Broad signals were observed in the 200-MHz ^{1}H NMR spectra of the complexes at 20 °C due to inversion of the thioether ligands. However, spectra recorded at lower temperatures enabled complete assignment of the signals. These data showed that signals due to the α-protons of the axial ligands are downfield of the corresponding signals of equatorial ligands, in contrast with previous observations. No ligand exchange was observed when dimethyl disulfide was added to solutions of the complexes at temperatures required to achieve coalescence of the NMR signals, indicating that ligand inversion occurs by a nondissociative mechanism.

Introduction

Organo sulfide complexes of rhodium, iridium, ruthenium, and other transition-metal halides are well-known.[1] For example, Chatt et al.[2,3] examined their catalytic properties and Allen and Wilkinson[4,5] studied their structural features. Although claims were made for a *fac* configuration,[6-9] Allen and Wilkinson,[5] using a combination of X-ray, NMR, dipole moment, and electronic spectral studies, clearly demonstrated that complexes of the type MX_3L_3 (M = Rh, Ir; X = Cl, Br, I; L = SMe_2, SEt_2, tetra-

(1) For a general review see: Murray, S. G.; Hartley, F. R. *Chem. Rev.* **1981**, *81*, 365.
(2) Chatt, J.; Leigh, G. J.; Storace, A. P.; Squire, D. A.; Starkey, B. J. *J. Chem. Soc. A* **1971**, 899.
(3) Chatt, J.; Leigh, G. J.; Storace, A. P. *J. Chem. Soc. A* **1971**, 1380.
(4) Allen, E. A.; Johnson, N. P.; Wilkinson, W. *J. Chem. Soc. D* **1971**, 804.
(5) Allen, E. A.; Wilkinson, W. *J. Chem. Soc., Dalton Trans.* **1972**, 613.
(6) Aires, B. E.; Fergusson, J. E.; Howarth, D. T.; Miller, J. M. *J. Chem. Soc. A* **1971**, 1144.
(7) Kauffman, G. B. *Inorg. Synth.* **1963**, *7*, 224.
(8) Fergusson, J. E.; Karran, J. D.; Seevaratnam, S. *J. Chem. Soc.* **1965**, 2627.
(9) Kauffman, G. B.; Tsai, J. H.; Kay, R. C.; Jørgenson, C. K. *Inorg. Chem.* **1963**, *2*, 1233.

0020-1669/88/1327-3526$01.50/0

hydrothiophene) have a *mer* configuration.

In the course of other studies[10] relating to the desulfurization of hydrocarbon oils containing organosulfur compounds, we prepared complexes between rhodium(III) halides and tetrahydrothiophene (tht) in an aqueous environment. Preliminary examination of these materials showed that they were identical with those complexes described previously.[4,5] However, the 200-MHz ^{1}H NMR spectra of our complexes showed significant differences compared to the spectra reported previously. Consequently, we carried out further investigations to confirm that our complexes were indeed identical with those reported by Allen and Wilkinson.[5]

This paper describes the ^{1}H NMR spectra of the complexes $RhX_3(tht)_3$ (X = Cl, Br, I) recorded at temperatures varying from 213 to 363 K, their ^{13}C NMR spectra, and the X-ray crystal structure of $RhCl_3(tht)_3$.

Experimental Section

Complexes. These were prepared as described previously[5] by refluxing the appropriate rhodium trihalide and a slight excess of tetrahydrothiophene in methanol for 15 min. Removal of the solvent yielded orange-red solids, which were crystallized from ethanol. All of the complexes gave satisfactory analytical data.

The chloro complex was also obtained by contacting an aqueous solution of rhodium trichloride with a 10-fold molar excess of tetrahydrothiophene. After a prolonged period at 3 °C (approximately 1 month), orange crystals had formed at the interface of this mixture. The analysis and spectral properties of these crystals matched those of the material obtained from the preparation in methanol.

X-ray Structure Determination. Crystal Data: $C_{12}H_{24}Cl_3RhS_3$, fw = 473.78; monoclinic, space group $P2_1/n$; a = 11.887 (2), b = 10.3168 (7), c = 15.237 (3) Å; β = 107.266 (9)°; V = 1784.4 (5) Å^3; Z = 4; ρ_o = 1.758 (3), ρ_c = 1.766 g cm^{-3} (21 °C; Mo Kα, λ = 0.710 69 Å, graphite monochromator); $F(000)$ = 960; μ(Mo Kα) = 16.98 cm^{-1}.

Intensity data were collected at room temperature on an Enraf-Nonius CAD4F diffractometer using the ω–2θ scan technique with a scan range of 1.5(0.66 + 0.347 tan θ)°. The intensity was calculated as $I = [P - 2(B1 + B2)]_Q$, where P is the central 64 steps of a 96-step scan, B1 and B2 are the background counts, and Q is the scan rate. The standard deviation of the intensity $\sigma(I) = [P + 4(B1 + B2)]^{1/2}Q$. Three standard reflections measured every 2500 s of X-ray exposure time showed no decomposition of the crystal had occurred during the data acquisition period. A total of 3108 unique reflections were measured for the octants $\pm h,+k,+l$ to a maximum θ = 25°, of which 2137 were considered observed ($F_o > 3\sigma(F_o)$). The data were corrected for background, Lorentz, and polarization effects, and an absorption correction was applied using the Gaussian method[11] with a 10 × 8 × 14 grid. The crystal possessed eight faces, namely {001}, {110}, and {101}. Transmission coefficients were found to vary from 0.620 to 0.674.

The coordinates of the Rh atom were determined by a three-dimensional Patterson synthesis. Structure factor and difference Fourier calculations revealed the positions of the remaining non-hydrogen atoms. The structure was refined by full-matrix least-squares techniques based on F, minimizing the function $\sum w(|F_o| - |F_c|)^2$, where w was $[\sigma^2(F_o) + 0.0002(F_o^2)]^{-1}$. All computations were performed by using the XRAY 76 system of programs[12] implemented on a Honeywell computer with a Multics operating system. Scattering factors for non-hydrogen atoms were those of Cromer and Mann,[13] and those for H were taken from Stewart et al.[14] Anomalous dispersion corrections were included for non-hydrogen atoms.[15] Hydrogen atoms were readily located from a difference Fourier map and included in the model in calculated positions (sp^3 C, C–H = 1.00 Å) with isotropic thermal parameters set to 1.1 times the U_{equiv} value of the atom to which they are bonded. Hydrogen parameters were not refined. The model converged for 2572 reflections (observed reflections plus those for which $I_c > 3\sigma(I_o)$) and 172 variables with the agreement factors $R = \sum(||F_o| - |F_c||)/\sum|F_o| = 0.027$ and $R_w = [\sum w(|F_o| - |F_c|)^2/\sum w|F_o|^2]^{1/2} = 0.034$. In the final cycle, the maximum shift/error was 0.05, the goodness of fit value was 0.97, and the largest peak of residual electron density was 0.47 e Å^{-3} and is of no chemical significance. An isotropic extinction correction could not be refined. Atomic coordinates and U_{equiv} values for the non-H atoms are given in Table I; bond angles and bond lengths are collected in Table II.

Table I. Positional Parameters (×10^4) and B_{eq} (Å^2 × 10) for the Non-Hydrogen Atoms of $RhCl_3(tht)_3$

atom	x/a	y/b	z/c	B_{eq}
Rh	−490.5 (3)	2053.0 (3)	2331.5 (2)	28
Cl(1)	923.4 (12)	2386.3 (12)	3767.4 (8)	41
Cl(2)	974.1 (10)	2040.1 (12)	1589.4 (9)	44
Cl(3)	−2001.1 (10)	2150.3 (11)	3032.7 (9)	39
S(1)	−1951.5 (10)	1800.2 (11)	929.9 (8)	32
S(2)	−316.9 (10)	−196.6 (11)	2519.7 (8)	33
S(3)	−631.2 (12)	4335.8 (11)	2233.4 (9)	40
C(1)	−3092 (4)	700 (5)	1034 (4)	43
C(2)	−3325 (5)	−230 (5)	240 (3)	47
C(3)	−2176 (6)	−533 (6)	116 (4)	59
C(4)	−1499 (5)	727 (7)	139 (4)	59
C(5)	−615 (4)	−697 (5)	3572 (4)	46
C(6)	405 (7)	−1538 (7)	4065 (5)	84
C(7)	1449 (6)	−1145 (7)	3887 (5)	76
C(8)	1244 (5)	−634 (5)	2943 (4)	51
C(9)	−1155 (4)	4943 (5)	1069 (4)	43
C(10)	−373 (5)	6104 (6)	1058 (4)	59
C(11)	823 (5)	5755 (6)	1551 (5)	62
C(12)	838 (5)	5050 (5)	2432 (4)	48

Table II. Bond Lengths (Å) and Angles (deg) for $RhCl_3(tht)_3$

Rh–Cl(1)	2.355 (1)	S(2)–C(5)	1.817 (6)
Rh–Cl(2)	2.341 (1)	S(2)–C(8)	1.831 (5)
Rh–Cl(3)	2.348 (2)	C(5)–C(6)	1.499 (9)
Rh–S(1)	2.333 (1)	C(6)–C(7)	1.407 (11)
Rh–S(2)	2.340 (1)	C(7)–C(8)	1.483 (10)
Rh–S(3)	2.363 (1)	S(3)–C(9)	1.809 (5)
S(1)–C(1)	1.812 (5)	S(3)–C(12)	1.836 (6)
S(1)–C(4)	1.830 (7)	C(9)–C(10)	1.519 (8)
C(1)–C(2)	1.505 (7)	C(10)–C(11)	1.444 (8)
C(2)–C(3)	1.466 (10)	C(11)–C(12)	1.521 (9)
C(3)–C(4)	1.525 (9)		
Cl(1)–Rh–Cl(2)	91.23 (5)	S(1)–C(1)–C(2)	107.0 (4)
Cl(1)–Rh–Cl(3)	90.14 (5)	C(1)–C(2)–C(3)	106.5 (4)
Cl(1)–Rh–S(1)	177.11 (5)	C(2)–C(3)–C(4)	108.7 (5)
Cl(1)–Rh–S(2)	91.05 (4)	C(3)–C(4)–S(1)	106.0 (4)
Cl(1)–Rh–S(3)	86.04 (4)	Rh–S(2)–C(5)	110.9 (2)
Cl(2)–Rh–Cl(3)	177.28 (5)	Rh–S(2)–C(8)	109.3 (2)
Cl(2)–Rh–S(1)	90.89 (5)	C(5)–S(2)–C(8)	93.6 (3)
Cl(2)–Rh–S(2)	90.13 (5)	S(2)–C(5)–C(6)	105.5 (5)
Cl(2)–Rh–S(3)	91.37 (5)	C(5)–C(6)–C(7)	111.4 (6)
Cl(3)–Rh–S(1)	87.67 (5)	C(6)–C(7)–C(8)	112.9 (5)
Cl(3)–Rh–S(2)	92.19 (5)	C(7)–C(8)–S(2)	106.7 (5)
Cl(3)–Rh–S(3)	86.38 (5)	Rh–S(3)–C(9)	113.9 (2)
S(1)–Rh–S(2)	90.91 (4)	Rh–S(3)–C(12)	110.1 (2)
S(1)–Rh–S(3)	91.95 (4)	C(9)–S(3)–C(12)	93.3 (2)
S(2)–Rh–S(3)	176.75 (4)	S(3)–C(9)–C(10)	104.5 (3)
Rh–S(1)–C(1)	111.3 (2)	C(9)–C(10)–C(11)	108.0 (5)
Rh–S(1)–C(4)	112.7 (2)	C(10)–C(11)–C(12)	109.3 (6)
C(1)–S(1)–C(4)	93.0 (3)	C(11)–C(12)–S(3)	106.5 (3)

NMR Spectra. ^{1}H NMR spectra were recorded at 200 MHz with use of 1.5 × 10^{-2} M solutions of the complexes in $CDCl_3$ on a Varian XL-200 FT spectrometer. The solvent was used as an internal lock, and the spectra were internally referenced to TMS. Proton-decoupled ^{13}C NMR spectra were recorded similarly at 50.3 MHz. These data are shown in Tables III and IV.

Results and Discussion

X-ray Studies. A single-crystal X-ray study was carried out on $RhCl_3(tht)_3$ using the methods described in the Experimental Section. An ORTEP[16] plot of the compound is given in Figure 1, and bond lengths and bond angles are given in Table II. The structure consists of discrete molecular units, and there are no

(10) Clark, P. D.; Dowling, N. I.; Lesage, K. L.; Hyne, J. B. *Fuel* **1987**, *66*, 1699.
(11) Using a modified program from P. Coppens, Crystallographic Computing Programs, State University of New York at Buffalo, Buffalo, NY.
(12) Stewart, J. M., Ed. Technical Report TR-446; Computer Science Center, University of Maryland: College Park, MD.
(13) Cromer, D. T.; Mann, J. B. *Acta Crystallogr., Sect. A: Cryst. Phys., Diffr., Theor. Gen. Crystallogr.* **1968**, *A24*, 321.
(14) Stewart, R. F.; Davidson, E.; Simpson, W. *J. Chem. Phys.* **1968**, *42*, 3175.
(15) *International Tables for X-ray Crystallography*; Kynoch: Birmingham, England, 1974.
(16) Johnson, C. K. ORTEP Report ORNL-3794; Oak Ridge National Laboratory: Oak Ridge, TN, 1965.

Table III. ^{1}H NMR Spectral Data[a,b]

		chem shift, δ			coupling constant, Hz	
	T, K	α_{ax}	α_{eq}	$\beta_{ax,eq}$	J_{ax}[c]	J_{eq}[c]
$RhCl_3(tht)_3$	213	2.86–3.0	2.86–3.00	2.04–2.20	12.7	12.7
		3.64–3.76	3.20–3.30	2.30–2.38		
	273	2.86–2.98	2.86–2.98	2.02–2.18	12.9	12.7
		3.70–3.84	3.24–3.36	2.28–2.38		
	323	2.90[d]	2.90[c]	2.02–2.18	*e*	*e*
		3.76[d]	3.28[c]	2.26–2.36		
$RhBr_3(tht)_3$	213	3.00–3.06	2.96–3.02	2.06–2.18	12.8	12.3
		3.83–3.90	3.34–3.40	2.24–2.32		
	273	2.97–3.04	3.0[d]	2.04–2.18	13.2	*e*
		3.90–3.96	3.4[d]	2.23–2.34		
	323	*d*	*d*	2.20–2.24	*e*	*e*
$RhI_3(tht)_3$	213	3.10–3.17	3.01–3.07	2.00–2.30	12.4	11.9
		4.09–4.15	3.42–3.48			
	273	3.11–3.15	3.24[d]	2.04–2.18	*e*	*e*
		4.13–4.16				
	323	3.60[d]	3.23[f]	2.10–2.22[f]	*e*	*e*

[a] Data at intermediate temperatures are available upon request. α and β refer to protons on carbons adjacent to and one atom removed from S atoms. [b] All signals occurred as multiplets. [c] Obtained from decoupled spectra. [d] Very broad signal of low intensity due to coalescence. [e] Unobtainable due to coalescence. [f] All signals have coalesced to a single peak.

Table IV. ^{13}C NMR Data[a] for $RhX_3(tht)_3$

	α-C[b]		β-C[b]	
X	ax	eq	ax	eq
Cl	40.06	38.47	30.12	29.97
Br	45.46	41.08	30.36	30.15
I	45.47	41.11	30.37	30.12

[a] In ppm relative to TMS. [b] α and β refer to carbon atoms adjacent to and one atom removed from the S atom of the tht ligands.

unusual intramolecular contacts as ligands do not approach closer than expected for the sum of van der Waals radii. The tht ligands twist with respect to each other (presumably to minimize contact) but to show a consistent geometry relative to specific planes within the Rh octahedral core. The relevant dihedral angles are as follows: 56.2° for the planes [S(1), C(1), C(4)] and [Rh, Cl(1), Cl(2), Cl(3), S(1)]; 61.6° for [S(2), C(5), C(8)] and [Rh, Cl(2), Cl(3), S(2), S(3)]; 57.9° for [S(3), C(9), C(12)] and [Rh, Cl(1), S(1), S(3)]. The data confirm that the complex has a meridional configuration. Rh–Cl, S–C, and C–C bond lengths are all considered normal. The Rh–S bond lengths varied between 2.334 and 2.365 Å, which fall within the range of values quoted for other rhodium–thioether complexes[1] (2.322–2.369 Å) and are comparable to the value obtained by summing the covalent radii (Pauling) for rhodium and sulfur. The bond angles around the sulfur atoms show a distorted-tetrahedral geometry due to their inclusion in a five-membered ring; the C–S–C "bite" angles fall in the range 93–94°, which is normal for tht. Overall the X-ray data suggest that there is predominantly σ-type bonding between the Rh(III) center and the sulfur ligands and that the lone pair of electrons on the sulfur atoms occupy an orbital with mostly sp^3 character.

^{1}H NMR Studies. Allen and Wilkinson[5] recorded the ^{1}H NMR spectra of the complexes $RhX_3(tht)_3$ (X = Cl, Br, I) at 306 K using a 100-MHz spectrometer and observed, for each complex, a multiplet at δ 2.1–2.25 for the protons β to the sulfur atom and two multiplets varying between δ 3.0 and 4.1, which were assigned to the protons α to the sulfur atom of the axial and equatorial tht ligands. With the advantage of a 200-MHz spectrometer and measurements at temperatures between 213 and 363 K it became apparent that the spectra were more complex and at the different temperatures it was possible to observe the effects of the inversion at sulfur for the tht ligands.

At 213 K, the signals due to protons α to the sulfur atom for the axial and equatorial tht ligands of all three complexes were

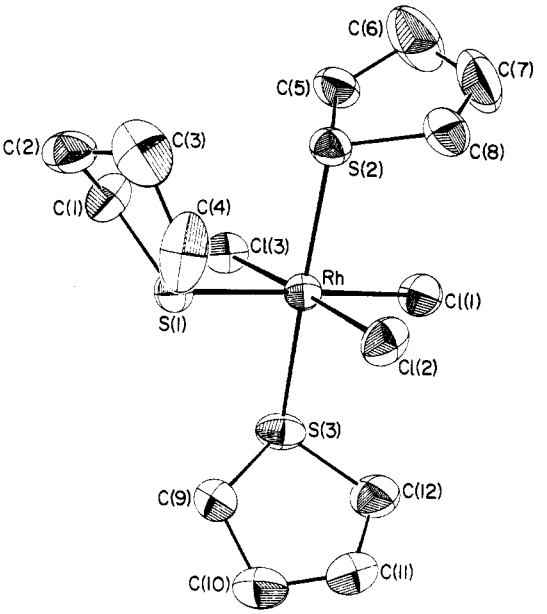

Figure 1. X-ray structure of $RhCl_3(tht)_3$.

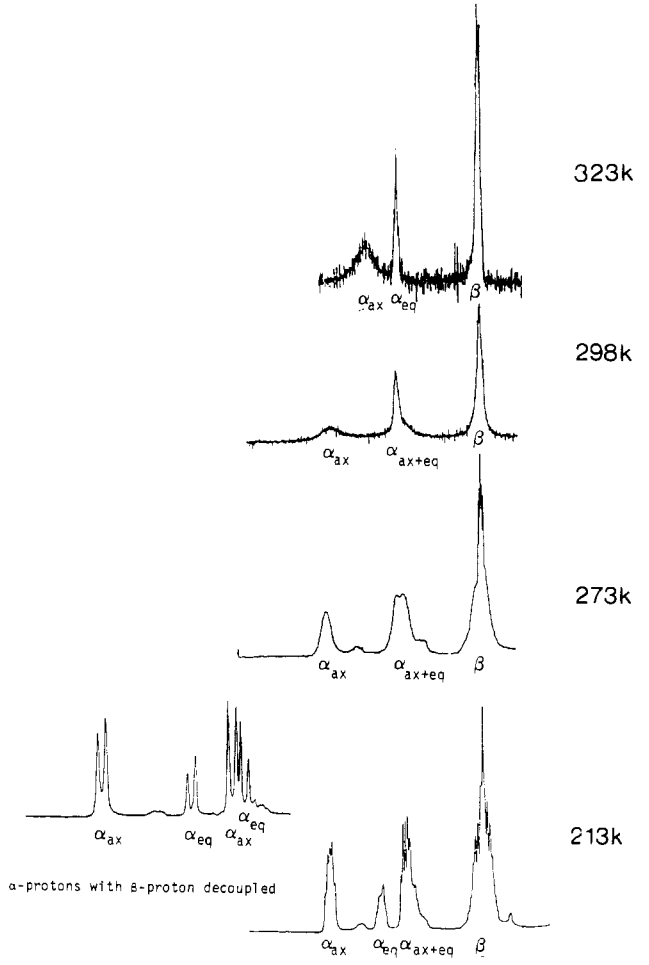

Figure 2. ^{1}H NMR spectra of $RhI_3(tht)_3$.

each observed as a pair of multiplets (see Table III for chemical shift data) with some overlap of the higher field signals. These resonances occurred in a 2:1 intensity ratio as expected for the *mer* configuration. Complex multiplets were observed for the β-protons of all three compounds at this temperature. At the lower temperatures, homonuclear decoupling of the β-proton multiplets reduced the α-protons to a pair of doublets for both the axial and equatorial ligands and this is illustrated in Figure 2 for the iodo complex. The reasons Allen and Wilkinson made different as-

signments will become obvious after discussion of spectra recorded at higher temperatures.

As the temperature was raised in stages from 213 to 363 K, first the resonances due to α-protons of the equatorial ligand coalesced followed by those of the axial ligands. This behavior was followed by the chloro, bromo, and iodo complexes, although the temperatures of coalescence varied. Between 273 and 323 K we observed spectra very similar to those described by Allen and Wilkinson in which the signals for the α-protons appeared as overlapping, partially coalesced multiplets. Thus, for the iodo complex (Figure 2) at 273 K two broad multiplets were observed for the α-protons with the highest field α-proton multiplet being twice as intense as the lower field multiplet. However, since we followed the progression of the spectra as the temperature was raised from 213 K, it was clear that the more intense higher field multiplet was comprised of signals from one multiplet of the α-protons of the axial ligands and the partially coalesced α-protons of the equatorial ligand. At 323 K, complete coalescence of the α-equatorial signals is seen along with partial coalescence of the α-axial signals (Figure 2).

Without the benefit of low-temperature spectra, Allen and Wilkinson[5] explained (erroneously) the 2:1 signal intensity for the α-proton signals by assigning the more intense signal to the α-axial protons and the less intense signal to the α-equatorial in order to fit the *mer* configuration. These workers studied a number of thioether complexes of rhodium and iridium, and in every case, except the tht complexes, they observed signals due to the α-protons of axial ligands (thioether ligands trans to one another) downfield of those for the equatorial ligands. However, they could not rationalize the spurious behavior when tht was the ligand. Our data (Table III) show that the α-protons for the axial ligands are downfield of the equatorial signals and thus the anomalous behavior noted by Allen and Wilkinson was simply due to difficulty in assigning the signals.

Attempts were made to determine the thermodynamic barriers to inversion of the tht ligands using the complete band-shape fitting techniques of Binsch.[17] Since the information necessary to use this method could not be extracted from a complete ^{1}H NMR spectrum, spectra simplified by decoupling the β-protons were obtained and signals due to the α-protons were fitted. Despite careful monitoring of the probe temperature ($\pm$1 K) and collection of data over a 150 K range, large errors (4–8 kJ mol^{-1}) in $\Delta G^{\ddagger}$ were obtained. Normally $\Delta G^{\ddagger}$ can be obtained within $\pm$0.5 kJ mol^{-1} and, although the reasons for larger errors in this work are not certain, it is possible that the decoupling procedure may have influenced band shapes through nuclear Overhauser effects.[18]

Values of $\Delta G^{\ddagger}$ ((53–65) $\pm$ (4–8) kJ mol^{-1}) and $\Delta H^{\ddagger}$ ((44–58) $\pm$ (2–5) kJ mol^{-1}) for the chloro, bromo, and iodo complexes were similar to those obtained for other transition-metal thioether complexes[19-21] and infer that the ligand inversion occurs by a nondissociative mechanism. This conclusion was supported experimentally since no ligand exchange was observed when dimethyl sulfide was added to the tht complexes at or below the coalescence temperatures. No further analysis of the thermodynamic data was attempted because of the experimental errors.

^{13}C NMR Studies. The proton-decoupled ^{13}C NMR spectra of the three complexes (Table IV) show the expected behavior in that each complex shows four signals due to the α- and β-carbons of the axial and equatorial tht ligands. The signals had a 2:1 intensity ratio, and thus the more intense ones were assigned to the axial ligands. The β-carbons occurred at very similar chemical shifts for all three complexes, but the α-carbons shifted to lower field as the halogen influence changed from Cl to Br to I. A similar behavior was noted for the chemical shift of the α-hydrogen in the proton spectra. Through-bond effects are unlikely to account for this trend since three bonds separate the halogen and α-carbons, and indeed, the trend should be reversed according to electronegativity effects. Consequently, we conclude that the downfield shifts are caused by through-space interactions between the α-carbons and the halogen substituents. Such interactions reinforce the possibility of nuclear Overhauser effects on the band-shape fitting procedures.

Acknowledgment. We wish to thank the Natural Sciences and Engineering Research Council of Canada and Alberta Sulphur Research Ltd. (Calgary) for financial assistance and B. King for preparation of the manuscript.

Supplementary Material Available: Table SI, listing thermal parameters for non-hydrogen atoms of $RhCl_3(tht)_3$, and Table SII, listing positional and thermal parameters of H atoms of $RhCl_3(tht)_3$ (2 pages); Table SIII, listing calculated and observed structure factors (14 pages). Ordering information is given on any current masthead page.

(17) Binsch, G. *J. Am. Chem. Soc.* **1969**, *91*, 1304.

(18) One reviewer pointed out that other attempts to obtain thermodynamic data from decoupled spectra also gave unreliable data.

(19) Abel, E. W.; Farrow, G. W.; Orrell, K. G. *J. Chem. Soc., Dalton Trans.* **1976**, 1160.

(20) Abel, E. W.; Farrow, G. W.; Orrell, K. G.; Sik, V. *J. Chem. Soc., Dalton Trans.* **1977**, 42.

(21) Abel, E. W.; Shamsuddin Ahmed, A. K.; Farrow, G. W.; Orrell, K. G. *J. Chem. Soc., Dalton Trans.* **1977**, 47.